Supplementary information

Content

1. Model description: individual-based simulations

To obtain a better understanding of how the density of founder cells affects assortment and competition in a biofilm, we constructed a highly simplified individual-based model of bacterial growth in a biofilm. Our conceptual model does not aim to accurately represent the biophysical processes occurring during biofilm formation, but is rather based on the simplest possible representation of biofilm growth allowing us to study the emergence of spatial segregation and assortment.

Cells are placed in a continuous two-dimensional space in which they can move around, which is placed on top of a discrete grid (i.e. the model therefore combines a continuous and discrete spacing; see Kreft et al. 1998). Each grid element contains nutrients that can be consumed by the cells localized on top of it. The nutrients that are consumed by a cell are converted into energy and can be used for cell division or EPS production. When cells have a sufficient amount of energy they can divide. The resulting daughter cell pushes away neighboring cells. During the process cells remain of a fixed size. The production of EPS stimulates further spreading, as explained in detail below. The discrete grid elements are used to model the spatial distribution and diffusion of nutrients and EPS. At every time step, cells can consume local nutrients, divide and produce EPS.

Initially each grid element is supplied with the same fixed amount N_{init} of nutrients (Fig. S1). Cells consume the locally available nutrients in accordance to Monod saturation kinetics (Aksnes & Egge 1991; Chubukov et al. 2013): $C(N) = V_{max} \cdot N / (N + K)$. C is the nutrient consumption rate, which depends on the local amount N of available nutrients. V_{max} is the maximum consumption rate, and K is the half saturation constant, which corresponds to that nutrient concentration at which half of the maximum consumption rate is obtained. The consumed nutrients are converted into energy (E), thereby assuming that one unit

of nutrients is converted to one unit of energy. When the energy level of a cell passes the threshold level E_d required for cell division, the cell divides with 50% probability per time unit. Upon cell division, a daughter cell is placed in a random direction from the mother cell at the minimal possible distance that prevents overlap with the mother cell, thereby potentially pushing aside neighboring cells that were already there (Fig. S2). Cell pushing is an iterative process, in which random cells are selected and examined for their overlap with neighboring cells. If a cell overlaps with its neighbor it is moved such the overlap between cells disappears (Fig. S2 and movie S1). If a cell overlaps with multiple neighbors the sum of movement vectors determines the eventual position of a cell. This iterative process is continued until none of the cells show any overlap with their neighbors. The energy remaining after cell division (i.e. after subtracting E_d) is divided equally among both daughter cells. Locally depleted nutrients can be replenished by diffusional exchange of nutrients between neighboring grid elements at rate D. The system boundaries of the two-dimensional grid are fixed.

To model the effects of the production of matrix components on biofilm growth, we assumed that a cell can produce five units of matrix per unit of energy (see E_m in Table S1; see Fig. S7, S8 and S9 show results for alternative matrix production costs). Matrix is secreted in the local environment and, like nutrients, diffuses in space at rate D (in the parameter sensitivity analysis we also examined alternative diffusion rates for matrix, D_{matrix}). To mimic matrix-mediated biofilm spreading we used the simple heuristic that effective cell size, the area a matrix surrounded cell occupies (S), increases linearly with the local matrix concentration: $S(M) = S_{min} + s \cdot M$, where S_{min} is the minimal effective cell size (i.e. cell size in the absence of matrix) and s the increase in effective cell size per unit matrix in the local environment, M. The minimal cell size is equal to one grid element (both occupying an area of one; the cell being round and the grid element being a square). In the presence of matrix components dividing cells push each other outward to a larger extent, potentially towards a region where still unexploited nutrients can be

accessed. Since matrix is costly to produce, cells that do not produce matrix, but are surrounded by cooperative cells, will have an advantage over matrix-producing cells. Our assumption that the effective cell size relates linearly to the concentration of matrix proteins is perhaps not realistic, but it is a simple and computationally efficient heuristic for colony spreading.

At the onset of biofilm growth cells are placed randomly within a limited radius (R_{init}) from the spatial center of the grid (Fig. S1). A biofilm is allowed to grow for a limited amount of time. Since the degree of assortment changes in time and space, biofilm formation was assumed to stop when 10% of space was occupied by cells (~1500 cells; T_{stop}). It is important to note that assortment would always emerge, also in the case of many founder cells, when biofilms would grow for an unlimited time period (Fig. S3 and Nadell et al. 2010). However, we know that colony biofilm growth in the lab is limited in time, possibly because the growth medium dries out. Therefore, we make a similar assumption in the model, by assuming the biofilm grows for a limited time period.

86

87 **Table S1**. Parameter settings under default conditions and for robustness analysis

Parameter	Description	Default value	Robustness analysis		
			Min	Max	Figure
Grid size	Dimensions of cellular grid used for surface	200 x 200	NA	NA	NA
S_{min}	Minimal cell size	1.0	0.5	15	S5, S6
N_{init}	Nutrients present at the onset of biofilm growth	10	2	18	S5, S6
V_{max}	Maximum nutrient consumption rate	2.5	1	4	S5, S6
K	Saturation constant	10	2	18	S5, S6
E_d	Energy required for one cell division	10	2	18	S5, S6
D_{matrix}	Diffusion rate of matrix	0.1	0.01	0.21	S5, S6
R_{init}	Distance from the center of the grid within which cells are placed at the onset of biofilm growth	5	2	22	S5, S6, S7, S8
T_{stop}	Time at which simulation is stopped (given by the % of total space that is occupied by cells)	10%	10% (Early)	40% (Late)	S5, S6
E_m	Energy required for the production of one unit of matrix	0.2	0.05	3	S7, S8
s	Increase in effective cell size per unit of matrix that is present in local environment	1	0.1	3	S7, S8

88

2. Robustness analysis

The model results shown in the main manuscript correspond to one parameter setting. In order to verify if the results are robust against parametric changes we performed a robustness analysis. The supplementary Figures S3, S5, S6, S7, S8 and S9 are part of this analysis. The analysis is divided in three parts: (1) Robustness of our methods for quantifying the degree of assortment in both the model and experiments; (2) Robustness of model outcome with respect to the structural model parameters, which affect the growth dynamics of biofilms; (3) Robustness of model outcome with respect to parameters affecting cooperation, like the costs and benefits of matrix production.

2.1. Assortment radius

In the model, the degree of assortment in a population of red- and green-labelled cells was defined by the difference between the average frequency of red cells surrounding a red focal cell and the average frequency of red cells surrounding a green focal cell. In the experiments, a similar measure was used, based on counting red and green pixels in images of a mixed population of green- and red-fluorescent bacteria (see Material and methods). The frequency of red cells (resp. red pixels) was determined for a disk with a certain radius around a focal cell (resp. pixel). It is intuitively obvious that the size of this radius affects the degree of assortment measured: when a very small radius is used, the cells/pixel in the disk around a focal cell/pixel will typically be descendants of the same progenitor and, hence, likely of the same color. In other words, the degree of assortment will be quantified as high when the measurement radius is very small. Conversely, when a very large radius is used most cells in the colony are included in the assortment measurement and, hence, the degree of assortment will be judged as low. Ideally, the size of the radius should correspond to the interaction range between cells (i.e. the distance at which an EPS-deficient cell can still profit from the presence of an EPS-producing cell).

Unfortunately, the interaction range is unknown for EPS production in *Bacillus subtilis*. We therefore investigated systematically how our experimental and simulation results were affected by the choice of measurement radius and the point in time where assortment is quantified.

Figure S3 shows how our assortment measure is affected by the measurement radius and the time of measurement in our simulations. In line with our expectations, the degree of assortment increases over time (Fig. S3a): at the onset of biofilm growth cells are randomly mixed (assortment level ≈ 0), while spatial patterning emerges after consecutive rounds of cell division. The rate of increase in assortment is comparable for the various measurement radii considered (Fig. S3a). At the moment where the measurement is taken, the degree of assortment measured decreases linearly with the measurement radius (Fig. S3b). In other words, our results are not biased due to the choice of a particular radius; qualitatively, any other radius would have yielded the same results.

Figure S4 shows that the same conclusion also applies to quantifying assortment in our experiments. As long as the measurement radius is neither too large nor too small, the results based on our method seem to be robust, at least qualitatively.

2.2. Structural model parameters

To check the robustness of our simulation results to changes in the model parameters, we conducted an extensive sensitivity analysis. In addition to the default set of parameter values for which the results are reported in the main text (Table S1), we considered for each parameter 20 alternative values (keeping all other parameter at their default values). For the eight "structural" parameters, S_{min}, N_{init}, V_{max}, K, E_d, D_{matrix}, R_{init} and T_{stop}, the results are shown in Figures S5 and S6 (see the figure legends for details). From these figures we can conclude that most parameters have a marginal effect on the level of assortment emerging during biofilm growth, with the exception of N_{init} (i.e. nutrients present at the onset of biofilm

growth) and E_d (i.e. minimal energy required for cell division). Specifically lower values of N_{init} (although not too low) and higher values of E_d result in stronger assortment. Both parameter changes exert their effect in the same way. By either decreasing N_{init} or increasing E_d cells become more nutrient limited, due to which it takes them longer to divide. In fact, it is the ratio between N_{init} and E_d that is of importance; when the cell division rate drops due to nutrient limitation (low values of N_{init}/E_d) the level of assortment increases. When N_{init} is however too low, the level of assortment decreases, because there are insufficient nutrients for biofilm growth (Fig. S6). Our results are in line with previous models that show as well that nutrient constrains facilitate the emergence of spatial segregation (Ben-Jacob et al. 1994; Nadell et al. 2010, 2013).

In conclusion, in our model the relationship between initial cell density and the degree of assortment in the mature biofilm is robust against substantial changes in the parameter settings. However, two parameters have not been explored: E_m and s (see Table S1). These parameters will be examined in the next section.

2.3. Costs and benefits of EPS production

We also verified the model results with respect to the costs and benefits of EPS production (i.e. matrix production). The cost of EPS production is defined by the energy a cell needs for the production of one unit of EPS (E_m). The benefit of EPS production results from the linearly relation between the local matrix concentration and the cell size (s). Colony spreading is facilitated if more cells secrete EPS. Here, we examine how the costs and benefits of EPS production affect the competition between EPS+ and EPS- cells in mixed biofilms (Fig. S7, S9) and the degree of assortment that emergences in these biofilms (Fig. S8, S9). The effects of the costs and benefits of EPS production are evaluated for different initial cell densities and cell spacing (quantified by the distance R_{init} from the center of the grid within which cells are placed at the onset of biofilm growth).

For each parameter combination, 10 replicate simulations were performed, which were started with – on average – an equal number of EPS+ and EPS- cells. Biofilms could subsequently grow and at the end of biofilm growth we determined the genotype frequencies. EPS production is said to be favored by selection if the average frequency of the EPS+ cells increases during competition, such that EPS+ cells are more abundant than the EPS- cells at the end of biofilm growth. Figure S8 shows that EPS is favored when the costs of EPS production are relatively low and the benefits high. This is in agreement with previous models made on the evolution of cooperation (Nowak 2006). For each combination of costs and benefits of EPS production, the relation between the initial cell density and the competitive advantage of EPS+ cells is as expected (Fig. 3): only for relatively low cell densities (i.e. high dilution levels) EPS production is favored. In agreement with our previous results (Fig. 2, S3, S4, S5), low cell densities result in high levels of assortment (Fig. S8). The costs and benefits of EPS production only marginally affect the overall degree of assortment (Fig. S8). Only when EPS production is very costly assortment levels drop. In that case, cells allocate their nutrients predominantly to EPS production instead of cell division, due to which there is little or no biofilm growth.

Based on Figure S7 and S8, we could as well determine how the level of assortment affects the parameter space in which EPS+ cells have a competitive advantage over EPS- cells. Figure S9 summarizes Figure S7 and S8 by showing the correlation between the level of assortment and the fraction of EPS+ cells at the end of biofilm growth. When the frequency of EPS+ cells at the end of biofilm growth is higher than 50%, EPS production is favored by selection, otherwise it is selected against. Each dot in Figure S9 corresponds to one of the parameter combinations shown in Figure S7 and S8 (averaging over 10 replicate simulations). As expected, high levels of assortment – associated with low initial cell densities – increase the number of parameter combinations for which EPS production is favored.

References

Aksnes DL, Egge JK. (1991). A theoretical model for nutrient uptake in phytoplankton. Mar. Ecol. Prog. Ser. 70:65–72.

Chubukov V, Uhr M, Le Chat L, Kleijn RJ, Jules M, Link H, et al. (2013). Transcriptional regulation is insufficient to explain substrate-induced flux changes in Bacillus subtilis. Mol. Syst. Biol. 9:n/a–n/a.

Ben-Jacob E, Schochet O, Tenenbaum A, Cohen I, Czirok A, Vicsek T. (1994). Generic modelling of cooperative growth patterns in bacterial colonies. Nature 368:46–49.

Kreft J-U, Booth G, Wimpenny JWT. (1998). BacSim, a simulator for individual-based modelling of bacterial colony growth. Microbiology 144:3275–3287.

Nadell CD, Bucci V, Drescher K, Levin SA, Bassler BL, Xavier JB. (2013). Cutting through the complexity of cell collectives. Proc. R. Soc. B Biol. Sci. 280:1–11.

Nadell CD, Foster KR, Xavier JB. (2010). Emergence of spatial structure in cell groups and the evolution of cooperation. PLoS Comput. Biol. 6:e1000716.

3. Supplementary figures and movies

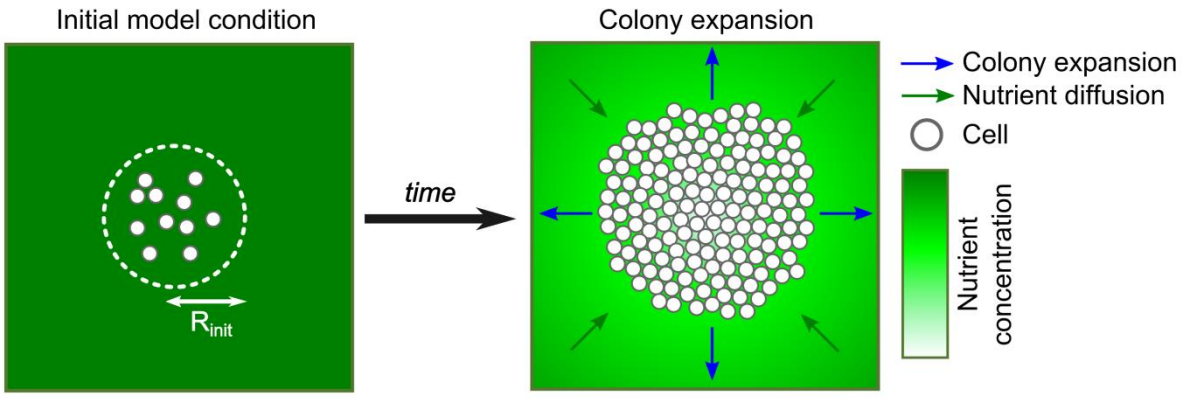

Figure S1. Model implementation: initial conditions and colony expansion. At the onset of colony growth each grid element contains the same initial amount of nutrients, N_{init}. The local nutrient concentration is reduced due to consumption during colony growth (dark green corresponds to nutrient rich spots and white to nutrient poor spots). At the onset of colony growth, cells are randomly placed within a circle of radius R_{init}. Over time, cell consume nutrients and – when having acquired sufficient energy (Fig. S2) – divide. As a result, the colony expands outwards in a lateral direction. In contrast, nutrients diffuse inward because they are consumed by cells in the center of the patch; resulting in a spatial gradient in which nutrients are most abundant on the edge of the colony and least abundant in the center of the colony. Cells spreading faster due to the presence of EPS acquire more nutrients and therefore have a fitness advantage.

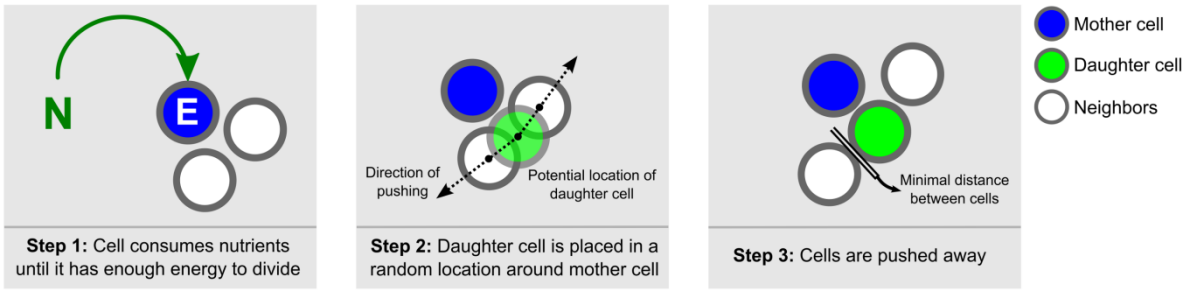

Figure S2. Model implementation: cell division and pushing. Cell division occurs in three computational steps, which all are part of the same time step in the simulation. First, cells have to convert nutrients to energy, until the minimal energy requirement for cell division, E_d, is reached. When cell division occurs (step 2), a daughter cell (green cell) of cell size S_{min} is placed in a random direction at the smallest possible distance from the mother cell (considering the effective cell size of the mother cell), irrespective of the occurrence of neighboring cells. From the position of the daughter cell the pushing effects on the surrounding cells are determined (see dotted arrows). In step 3, cells are placed away from the newly emerged daughter cell with a minimal distance of 0.03 (in terms of grid units). We use a small distance between cells after pushing to speed up the simulations. The process of cell pushing is continued by picking random cells that overlap with their neighbors and moving them around, until none of the cells overlap with their neighboring cells.

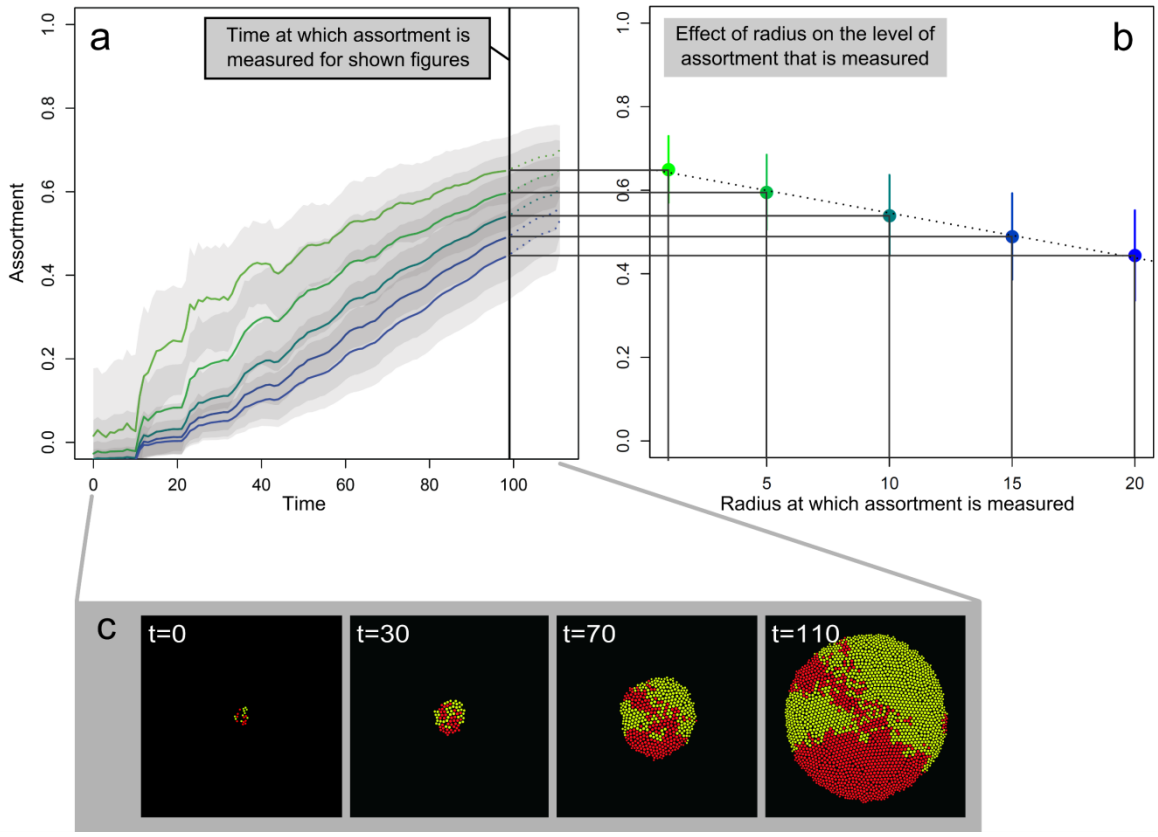

Figure S3. Change of assortment level in time and space. The dynamics of colony expansion results in the spatial segregation of cells, as becomes apparent from a time-course of colony growth (c). The level of assortment increases in time (a) and it decreases with the radius (see Material and methods) at which assortment is measured (b). Simulations shown in this figure are started with 20 cells and have the same parameter settings as the simulations in the main manuscript. The lines in (a) and the dots in (b) correspond to the average assortment level and the transparent grey areas in (a) and the error bars in (b) correspond to the standard deviation in assortment level (n=10 per treatment). The dotted line in (b) is a linear regression on the simulation data ($R^2 = 0.39$; $P < 10^{-6}$).

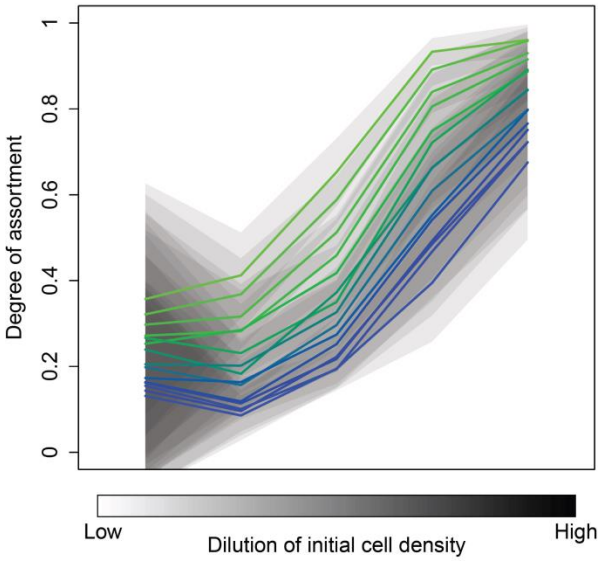

Figure S4. Effect of measurement radius on the relationship between initial cell density and spatial segregation in mature biofilms. Figure 2b in the main text reports how the degree of assortment in a biofilm after three days of growth depends on the initial cell density. In this figure, assortment was quantified by measuring the pixel density of red-and green fluorescent pixels in a disk with a radius of 50 pixels around a sample of focal pixels (see Material and methods). In the present figure, the same results are presented, but now based on a spectrum of circle radii, ranging from 5 pixels (upper green line) to 75 pixels (lower blue line). Incremental steps of 5 pixels are used for the different lines, with a total of 15 radii. The colored lines are the average assortment levels, while the grey polygons show the associated standard deviation.

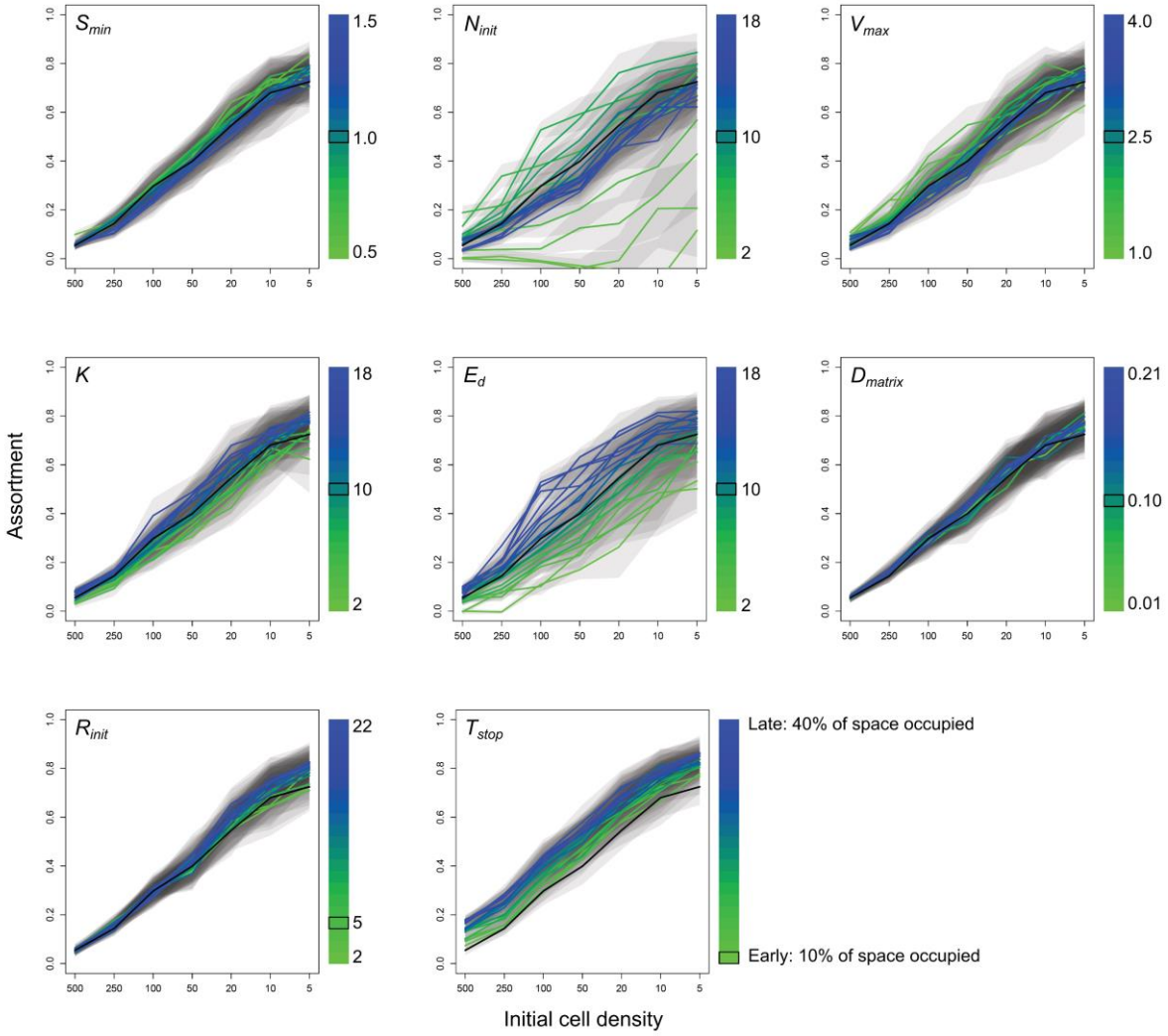

Figure S5. Effect of individual model parameters on the relationship between initial cell density and degree of assortment in mature biofilms. Figure 2a in the main text reports how in our model the degree of assortment in a mature biofilm depends on the initial cell density. This figure is based on the default parameter configuration (Table S1). The plots in the present figure illustrates for each of the model parameters S_{min}, N_{init}, V_{max}, K, E_d, D_{matrix}, R_{init} and T_{stop} how this relationship is affected by a change in the corresponding parameter value. Simulations were initiated with 5, 10, 20, 50, 100, 250 or 500 cells. The x axes show the initial cell numbers in the reversed order (from 500 to 5) like done for figure 2a. That is, Figure 2a shows the dilution levels on the x-axis, which inversely relate to the initial cell

numbers. For each parameter, 10 simulations per initial cell density were run for 21 different values of the parameter (keeping all other parameters at their default values). The scale to the right of each plot illustrates the linear range of parameter values tested, including the minimal value (green), the maximal value (blue), and the default value (slider box) of each parameter. The lines in the plots connect the mean levels of assortment measured, and the associated polygons indicate the corresponding standard deviations. Line colors (running from green to blue) indicate the corresponding value of the parameter considered.

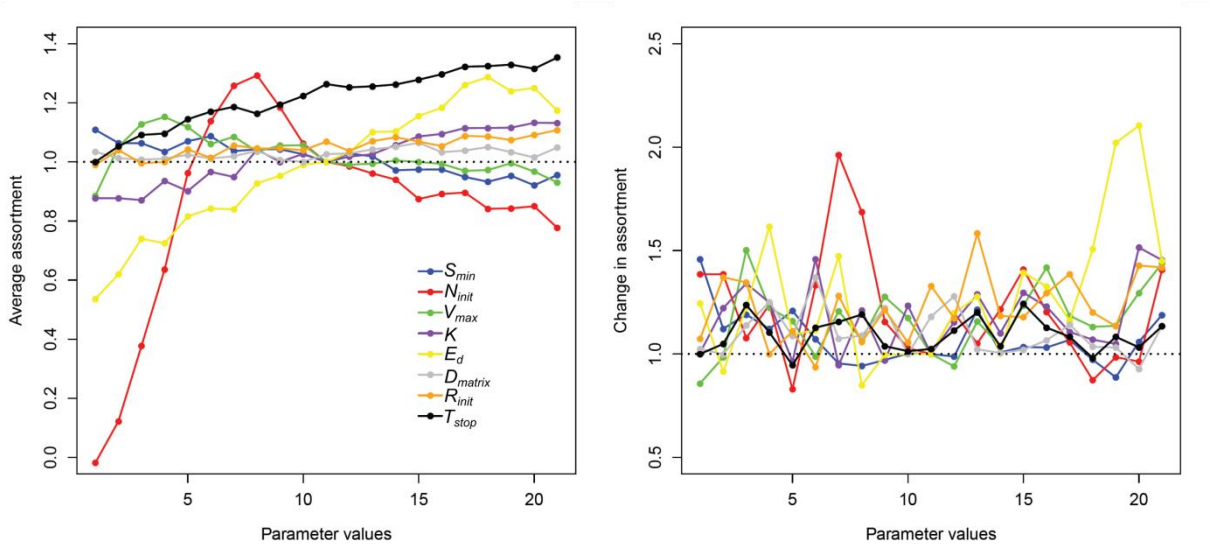

Figure S6. Effect of individual model parameters on the average degree of assortment and the change of assortment with initial cell density. For each of the eight model parameters considered in Fig. S5, the two plots summarize (a) the effect of each parameter on the degree of assortment, averaged over the seven initial cell density treatments considered in the simulations underlying Fig. S5, and (b) the effect of each parameter on the maximal change in assortment across the seven initial cell density treatments. The x-axis corresponds to the 21 values of each model parameter (see legend to Fig. S5); the assortment measures on the y-axis are normalized with respect to the default value of each parameter (see Table S1).

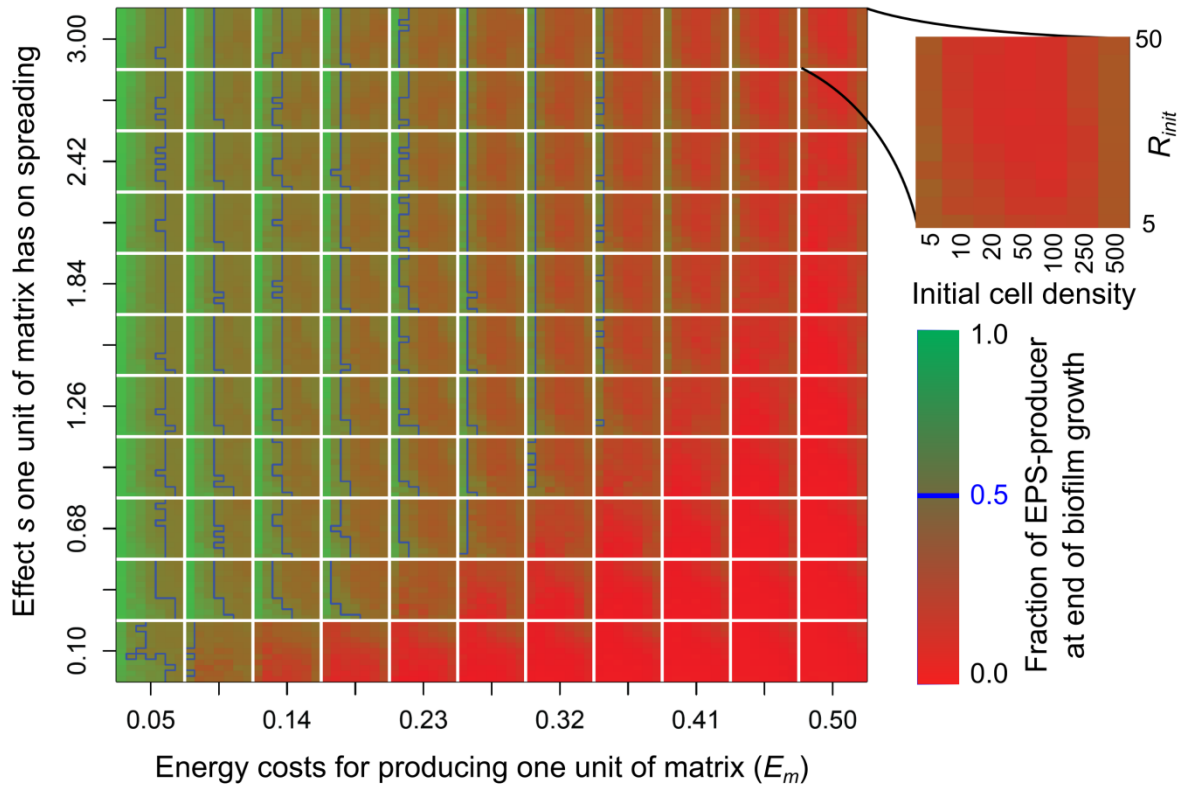

Figure S7. Effects of costs and spreading benefits of EPS production on the outcome of competition in our simulation model. The composite panel illustrates the outcome of competition between EPS+ cells (green) and EPS- cells (red) as a function of the costs of EPS production (quantified by the energy required E_m for the production of one unit of EPS), the effect s one unit of matrix has on spreading (i.e. spreading benefits), the initial cell density, and the initial spacing of cells (quantified by the distance R_{init} from the center of the grid within which cells are placed at the onset of biofilm growth). The shades of red and green indicate the average frequency of EPS+ cells at the end of biofilm growth: red correspond to low frequencies and green to high frequencies. The blue line shows the 50% boundary, in which EPS+ and EPS- cells are equally abundant at the end of biofilm growth. The main focus of the figure is on the costs (major horizontal axis) and spreading benefits (major vertical axis) of EPS production. Within these major axes, the initial cell density and R_{init} is varied as well. In total, almost 10,000 parameter

combinations were tested; for each parameter combination the average outcome of 10 replicate simulations is shown.

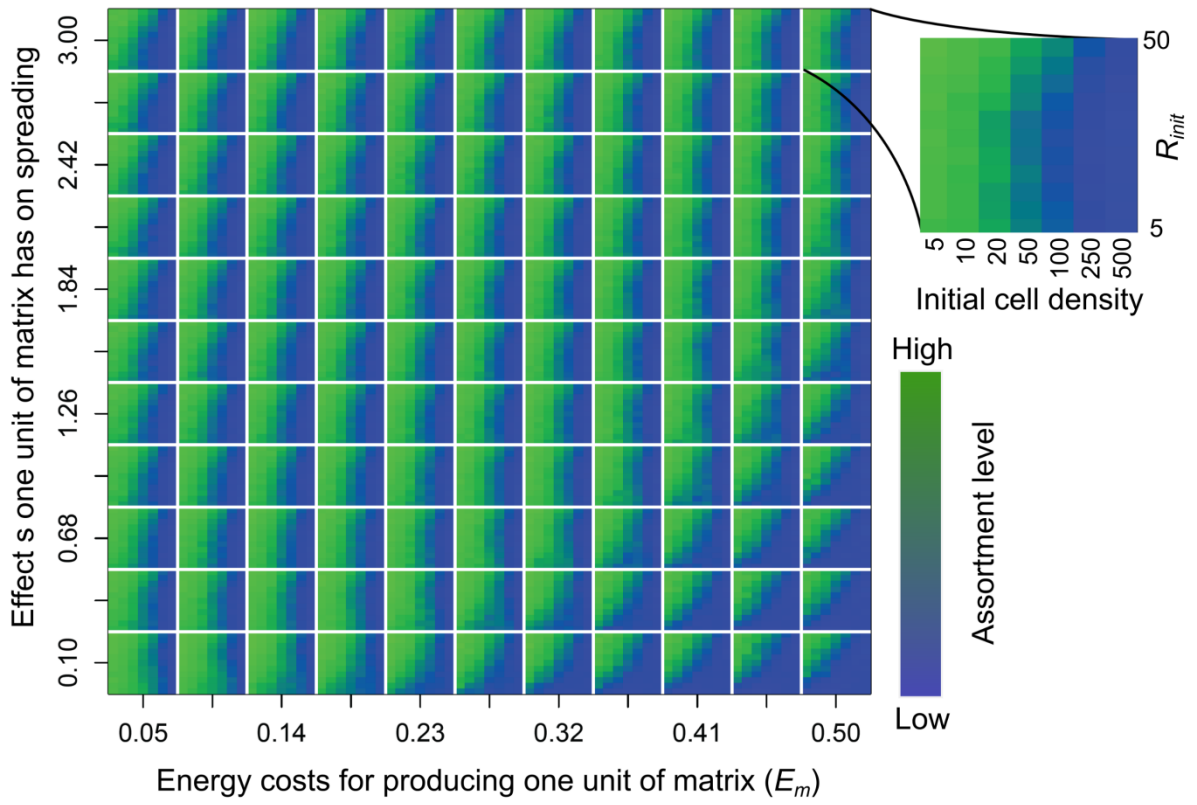

Figure S8. Effects of costs and spreading benefits of EPS production on spatial assortment in our simulation model. The composite panel illustrates the level of assortment in (EPS+/EPS-) mixed biofilms: blue is a low degree of assortment and green a high degree of assortment at the end of biofilm growth. The parameter conditions in this plot are the same as for Figure S7. Each parameter combination shows the average level of assortment for 10 replicate simulations.

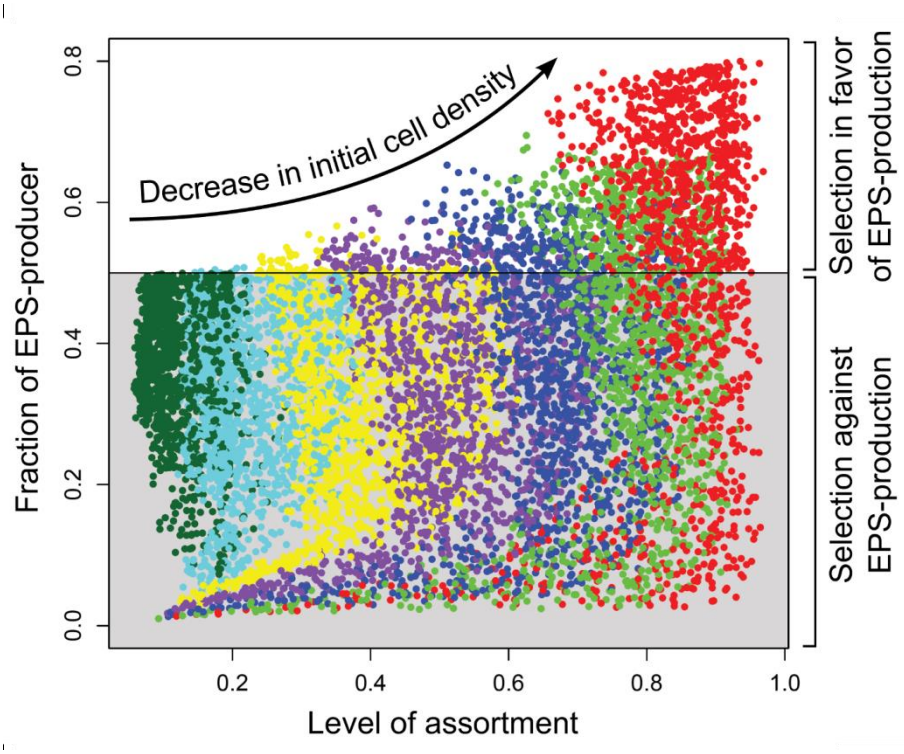

Figure S9. Relationship between initial cell density, cell assortment, and the selective advantage of EPS production. This figure summarizes the simulation results in Figures S7 and S8. Each dot corresponds to the average assortment level and the relative frequency of EPS producing cells (based on 10 replicates) achieved for one of the about 10,000 parameter combinations investigated. The colors indicate the initial cell number: 5 (red), 10 (green), 20 (blue), 50 (purple), 100 (yellow), 250 (cyan) and 500 (dark green). Given that each simulation is initiated with an equal number of EPS+ and EPS- cells, EPS production is favored by selection when the fraction EPS+ cells is higher than 0.5 at the end of biofilm growth, while otherwise it is selected against.

308

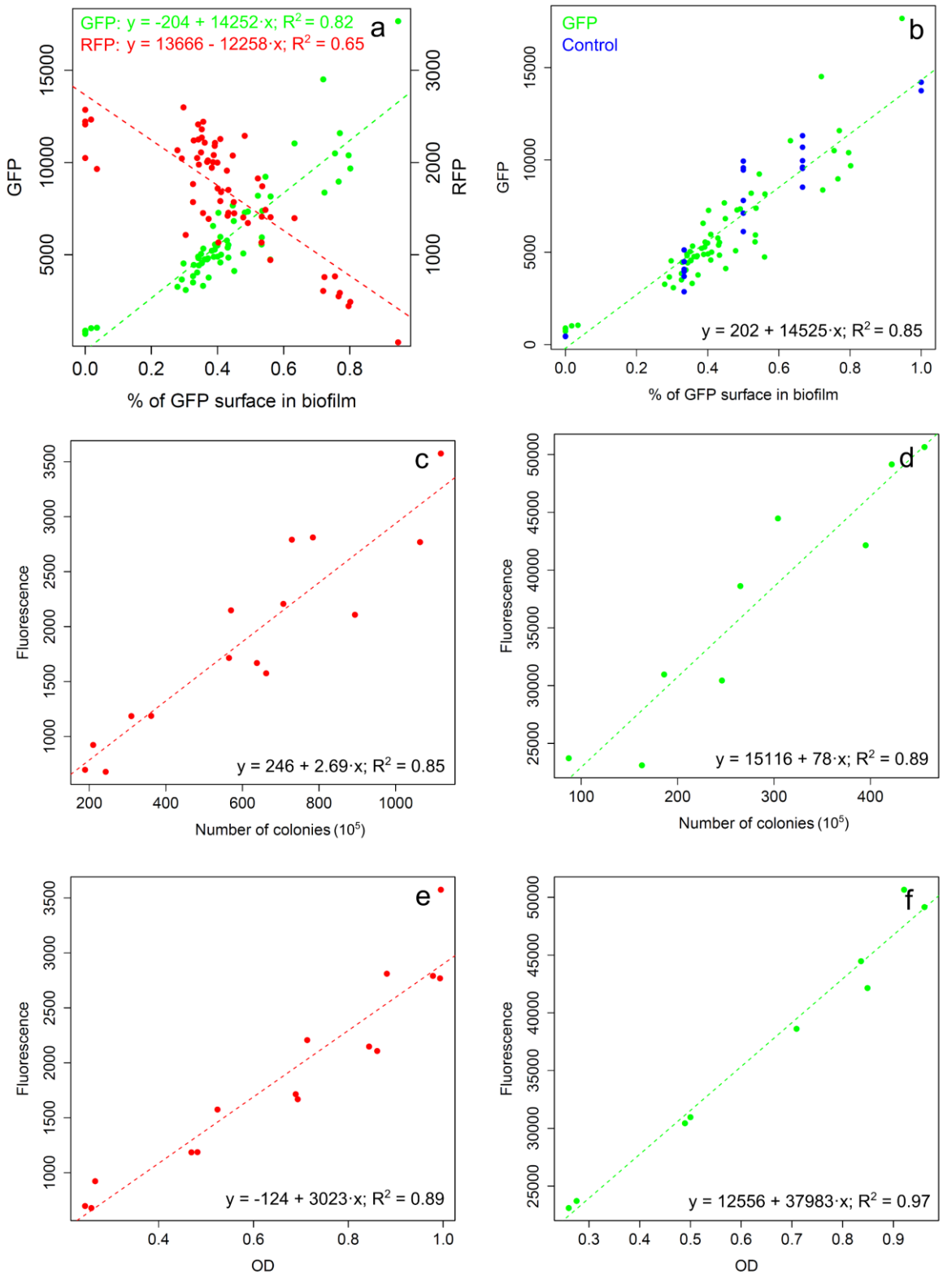
GFP: y = -204 + 14252·x; R² = 0.82
RFP: y = 13666 - 12258·x; R² = 0.65
a
GFP
RFP
% of GFP surface in biofilm
GFP
Control
b
y = 202 + 14525·x; R² = 0.85
% of GFP surface in biofilm
c
Fluorescence
y = 246 + 2.69·x; R² = 0.85
Number of colonies (10⁵)
d
Fluorescence
y = 15116 + 78·x; R² = 0.89
Number of colonies (10⁵)
e
Fluorescence
y = -124 + 3023·x; R² = 0.89
OD
f
Fluorescence
y = 12556 + 37983·x; R² = 0.97
OD

309

Figure S10. The abundance of a strain in the population is proportional to the fraction of biofilm surface it occupies. (a) The abundance of a strain in relation to the percentage of biofilm surface it occupies. Biofilms were inoculated by two eps^+ strains, each tagged with another fluorescent marker (GFP and RFP). The percentage of green fluorescent biofilm surface, after 3 days of growth, correlates with the overall green (linear regression: intersect = -204.9 ± 389.5 (SE), $P_{intersect}$=0.6, slope = 14251.8 ± 841.4, $P_{slope} < 2 \cdot 10^{-16}$, $R^2 = 0.82$, $F_{(1,61)} = 286.9$, $P < 10^{-15}$) and red fluorescence intensity (linear regression: intersect = 13666 ± 528, $P_{intersect} < 2 \cdot 10^{-16}$, slope = -12258 ± 1140, $P_{slope} = 1.05 \cdot 10^{-15}$, $R^2 = 0.65$, $F_{(1,61)} = 115.5$, $P < 10^{-14}$) in the population after biofilm dissection. Every biofilm corresponds to two data points: one shows the green fluorescence intensity and the other one the red fluorescence intensity. (b) Control experiment in which purely GFP and RFP expressing biofilms were mixed in fixed proportions before biofilm dissection (the mixes where made such that the percentage of GFP was 33%, 50% or 66%). This control data (blue) is superimposed on green fluorescent data from figure (a) and confirms the pattern found in co-cultured biofilms (linear regression on blue and green dots: intersect = -202.1 ± 323.0, $P_{intersect} = 0.5$, slope = 14525 ± 660.3, $P_{slope} < 2 \cdot 10^{-16}$, $R^2 = 0.85$). The green and red fluorescence intensity at the population level correlate with the number of, respectively, (c) green and (d) red fluorescent cells in the population ((c) linear regression: intersect = 246.6 ± 209.3, $P_{intersect}$=0.26, slope = 2.69 ± 0.3, $P_{slope} = 1 \cdot 10^{-6}$, $R^2 = 0.85$, $F_{(1,13)} = 73.7$, $P = 1 \cdot 10^{-4}$; (d) linear regression: intersect = 15116.5 ± 3202, $P_{intersect}=2 \cdot 10^{-3}$, slope = 78.2 ± 10.5, $P_{slope} = 1 \cdot 10^{-6}$, $R^2 = 0.89$, $F_{(1,7)} = 55.21$, $P < 10^{-3}$) and the optical density of (e) green and (f) red fluorescent cell cultures at 600 nm, OD_{600} ((e) linear regression: intersect = -123.8 ± 201.2, $P_{intersect}$=0.55, slope = 3023 ± 283.5, $P_{slope} = 8.5 \cdot 10^{-8}$, $R^2 = 0.89$, $F_{(1,13)} = 113.7$, $P < 10^{-7}$; (f) linear regression: intersect = 12556 ± 1501, $P_{intersect} = 6.9 \cdot 10^{-5}$, slope = 37983 ± 2165, $P_{slope} = 4.8 \cdot 10^{-7}$, $R^2 = 0.97$, $F_{(1,7)} = 307.9$, $P < 10^{-6}$).

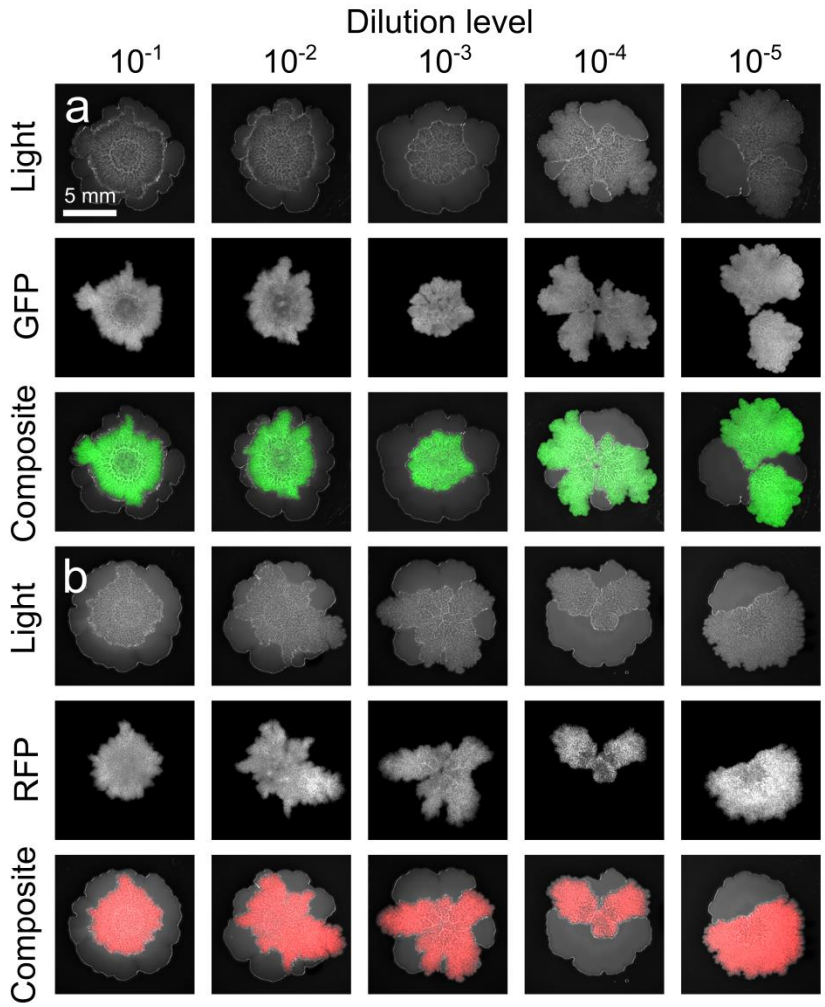

Figure S11. Images of spatial segregation between EPS producing and deficient cells. Five dilution levels where examined: 10^{-1}, 10^{-2}, 10^{-3}, 10^{-4}, 10^{-5}. (a) co-culture of eps^- and GFP-labeled eps^+ cells. From the top to bottom row images: light, GFP and composite images are shown. (b) co-culture of eps^- and RFP-labeled eps_{in} cells in the presence of 0.025 mM IPTG. From the top to bottom row images: light, RFP and composite images are shown. The fried-egg pattern that is observed at the lowest dilution level when co-culturing EPS producing and deficient strains cannot be reproduced by the mathematical model. Furthermore, EPS producing strains also partly overgrow the EPS deficient strain. The scale bar is equal to 5 mm.

Movie S1. Colony growth and the emergence of assortment in model. Example of colony growth for the parameter settings described in the Model description above. At the onset of biofilm growth, cells are randomly labeled with either a green or red color. All cells are assumed to produce EPS. The simulation is continued for a longer time than the simulations of the results shown in the manuscript, to illustrate the emergence of assortment in time.

Movie S2. Time-lapse movie of biofilm growth under standard culturing conditions. Mix of green-fluorescent (movie S1a) and red-fluorescent (movie S1b) EPS producing cells when grown for 3 days. Each fluorescent channel is shown in a separate movie, but both belong to the same biofilm. Movie frames are taken every 15 minutes for a period of three days.